Arch Pharm Res Vol 27, No 10, 1001-1008, 2004

Archives of Pharmacal Research
http://apr.psk.or.kr

3D QSAR Studies on Cinnamaldehyde Analogues as Farnesyl Protein Transferase Inhibitors

Nack-Do Sung, Young-Kwon Cho, Byoung-Mog Kwon[1], Kwan Hoon Hyun[2], and Chan Kyung Kim[2]

Division of Applied Biology & Chemistry, College of Agricultural & Life Sciences, Chungnam National University, Daejeon 305-764, [1]Korea and Anti-biotic Material RU, Korea Research Institute of Bioscience and Biotechnology, Daejeon 306-020, and [2]Department of Chemistry, Inha University, Inchon 402-751, Korea

(Received June 28, 2004)

Three-dimensional quantitative structure-activity relationship (3D-QSAR) studies on 59 cinnamaldehyde analogues as Farnesyl Protein Transferase (FPTase) inhibitors were investigated using comparative molecular field analysis (CoMFA) with the PLS region-focusing method. Forty-nine training set inhibitors were used for CoMFA with two different grid spacings, 2Å and 1Å. Ten compounds, which were not used in model generation, were used to validate the CoMFA models. After the PLS analysis, the best predictive CoMFA model showed that the cross-validated value (r^2_{cv}) and the non-cross validated conventional value (r^2_{ncv}) are 0.557 and 0.950, respectively. From the CoMFA contour maps, the steric and electrostatic properties of cinnamaldehyde analogues can be identified and verified.

Keywords: 3D-QSAR, CoMFA, Cinnamaldehyde inhibitors, Farnesyl protein transferase.

INTRODUCTION

A New inhibitor of farnesyl protein transferase (FPTase), 2-hydroxycinnamaldehyde, is isolated from the edible herb of cinnammon bark (*Cinnammoum Cassia* Blume) (Kwon *et al.*, 1996). It has been structurally modified in various positions: α,β-saturation on the olefinic moiety of the 2-hydroxycinnamaldehyde, functional group substitutions on the *ortho*, *meta* and *para* moieties and change of the carbonyl moiety to alcohol and acid functions. In the beginning of structure-activity relationships (SAR) study, *ortho*-substituted cinnamaldehydes were the main priority in structure modification, but it was later found that other substituents in the phenyl backbone show notable activity (Cho *et al.*, 2002).

Prenylation is a type of lipid modification involving the covalent addition of either farnesyl (15-carbon) or more commonly geranylgeranyl (20-carbon) isoprenoids *via* thioether linkages to cysteine residues at or near the C terminus of intracellular proteins. The attached lipid is required for proper function of the modified protein either as a mediator of membrane association or as a determinant for specific protein-protein interactions (signal transduction). Prenylated proteins play crucial roles in such vital cellular processes as signal transduction and intracellular trafficking pathways. These isoprenoid additions to proteins have been identified not only in mammalian systems but also in eukaryotes. Many inhibitors of protein prenylation especially in farnesyl transferase have been quite successful against human cancers with an understanding of the above mentioned mechanistic information (Adari *et al.*, 1988; Choo *et al.*, 2003; Gibbs *et al.*, 1994; Knight *et al.*, 1995; Lodish *et al.*, 1995; Schweins *et al.*, 1995; Qian *et al.*, 1994; Wu *et al.*, 1994).

Currently the inhibitors being designed or purified in academia and industry to new anticancer molecules that can specifically inhibit FPTase can be classified (Pedretti *et al.*, 2002) as (1) Non-specific (2) Zn^{2+} shielding (3) peptidomimetic (4) and farnesyl pyrophosphate (FPP) mimetic (Sung *et al.*, 2003). A cinnamaldehyde analogue is a unique example of a novel non-peptide, nonsulfhydryl containing FPTase inhibitor. Furthermore, these natural and edible herb originated materials may have more opportunities to be adapted to curative and/or substituted drugs in long term treatments.

In the beginning trials of the syntheses, we reported other biological information such as angiogenesis (Kwon *et al.*, 1997) in 1997 and *in vitro* cytotoxicity (Kwon *et al.*,

Correspondence to: Chan Kyung Kim, Department of Chemistry, Inha University, Inchon 402-751, Korea
Tel: 82-32-860-7684, Fax: 82-32-867-5604
E-mail: kckyung@inha.ac.kr

1998) in 1998 from the 19 kinds of cinnamaldehyde moieties.

In this work, a 3D QSAR study was performed using CoMFA that can elucidate steric and electrostatic properties with structural variations using 59 FPTase inhibitors, which have been synthesized and measured for their biological activity.

MATERIALS AND METHODS

Biological activity measurements

FPTase inhibitory activity was measured by Scintillation Proximity Assay (SPA) method (Reiss *et al.*, 1990) and the FPTase used in the experiment was separated from a rat. Enzyme activity was determined based on the degrees of the [^{3}H] farnesyl group transfer from the [^{3}H] farnesyl pyrophosphate to the Biotin-KKKSKTKCVIM peptide using liquid scintillation counter (LSC). To measure the inhibitory activity, enzyme solution was diluted up to final concentration of 10% DMSO after mixing an inhibitor solution dissolved in DMSO solvent. The inhibition (%) was calculated from eq. (1)

$$\text{Inhibition}(\%)=\left(1-\frac{\text{Sample(cpm)}-\text{Blank 2(cpm)}}{\text{Control(cpm)}-\text{Blank 1(cpm)}}\right)\times 100 \quad (1)$$

where, Blank 1 is cpm value with sample and the enzyme, Blank 2 is cpm value of sample without enzyme and Control is cpm value of enzyme without sample. The molar concentration of 50% inhibition activity (IC_{50}) was obtained by performing experiments at different concentrations and pI_{50} was calculated from eq. (2).

$$pI_{50} = -\log(IC_{50}/M.W \times 1000) \quad (2)$$

MOLECULAR MODELING

Date set for analysis

To perform the ligand-based QSAR study, 49 FPTase training set inhibitors were selected and their molecular structures and pI_{50} values are summarized in Table I. Two important dihedral angles (θ, φ) were depicted in the structure of the cinnamaldehyde.

Table I. FPTase inhibitory activities of *ortho*, *meta* and *para* substituted cinnamaldehyde derivatives

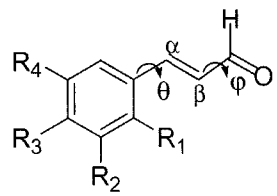

No.	R_1(*ortho*)	R_2(*meta*)	R_3(*para*)	R_4(*meta*)	pI_{50}[a]
1	H-	H-	H-	H-	2.27
2	HO-	H-	H-	H-	3.34
3	CH_3O-	H-	H-	H-	3.24
4	$CH_3CH_2CH_2O$-	H-	H-	H-	3.44
5	$CH_3CH_2CH(CH_3)O$-	H-	H-	H-	3.30
6	$CH_3OC(=O)CH_2O$-	H-	H-	H-	3.51
7	$(CH_3)_3CC(=O)CH_2O$-	H-	H-	H-	3.49
8	4-F-$C_6H_4C(=O)CH_2O$-	H-	H-	H-	3.27
9	$C_6H_5CH_2CH_2O$-	H-	H-	H-	3.38
10	$C_6H_5CH_2O$-	H-	H-	H-	3.68
11	2-OCH_3-$C_6H_4CH_2O$-	H-	H-	H-	5.56
12	3-OCH_3-$C_6H_4CH_2O$-	H-	H-	H-	3.95
13	4-OCH_3-$C_6H_4CH_2O$-	H-	H-	H-	3.41
14	2-NO_2-$C_6H_4CH_2O$-	H-	H-	H-	3.57
15	4-NO_2-$C_6H_4CH_2O$-	H-	H-	H-	3.03
16	4-CH_3-$C_6H_4CH_2O$-	H-	H-	H-	3.37
17	4-Br-$C_6H_4CH_2O$-	H-	H-	H-	3.43
18	4-Cl-$C_6H_4CH_2O$-	H-	H-	H-	3.48
19	4-CF_3-$C_6H_4CH_2O$-	H-	H-	H-	3.59

Tablel I. Continued

No.	R_1(*ortho*)	R_2(*meta*)	R_3(*para*)	R_4(*meta*)	pI_{50}[a]
20	2, 5-$(CH_3)_2$-$C_6H_3CH_2O$-	H-	H-	H-	3.58
21	4-Cl, 2-NO_2-$C_6H_3CH_2O$-	H-	H-	H-	3.21
22	3, 4-$(CH_3)_2$-$C_6H_3CH_2O$-	H-	H-	H-	3.62
23	2, 4-$(Cl)_2$-$C_6H_3CH_2O$-	H-	H-	H-	3.48
24	6-F, 2-Cl-$C_6H_3CH_2O$-	H-	H-	H-	3.58
25	3, 5-$(CH_3O)_2$-$C_6H_3CH_2O$-	H-	H-	H-	3.62
26	5-NO_2, 2-OCH_3-C_6H_3-CH_2O	H-	H-	H-	3.43

No.	R_1(*ortho*)	R_2(*meta*)	R_3(*para*)	R_4(*meta*)	pI_{50}
27	$C_6H_5C(=O)O$-	H-	H-	H-	3.19
28	2-Cl-$C_6H_4C(=O)O$-	H-	H-	H-	3.85
29	4-Cl-$C_6H_4C(=O)O$-	H-	H-	H-	3.55
30	2, 4-$(Cl)_2$-$C_6H_3C(=O)O$-	H-	H-	H-	3.57
31	3, 5-$(Cl)_2$-$C_6H_3C(=O)O$-	H-	H-	H-	3.56
32	4-CN-$C_6H_4C(=O)O$-	H-	H-	H-	3.56
33[b]	$OC_4H_3C(=O)O$-	H-	H-	H-	3.75
34	$CH_3C(=O)$-	H-	H-	H-	3.26
35	H-	HO-	H-	H-	2.77
36	H-	H-	HO-	H-	2.47
37	$CH_3C(=O)O$-	H-	H-	H-	3.44
38	Cl-	H-	Cl-	H-	3.79
39	H-	CH_3O-	CH_3O-	H-	3.20
40	H-	NH_2-	Cl-	H-	3.02
41	H-	CH_3O-	2-CH_3O-$C_6H_4CH_2O$-	CH_3O-	3.70
42	H-	CH_3O-	5-NO_2, 2-CH_3O-$C_6H_3CH_2O$-	CH_3O-	3.51
43	H-	H-	Cl-	2-Cl-$C_6H_4C(=O)NH$-	4.17
44	H-	H-	Cl-	4-Cl-$C_6H_4C(=O)NH$-	3.51
45	H-	H-	Cl-	2, 4-$(Cl)_2$-$C_6H_3C(=O)NH$-	3.55
46	H-	H-	Cl-	4-CN-$C_6H_4C(=O)NH$-	3.31
47	H-	H-	Cl-	$OC_4H_3C(=O)NH$-	3.50
48	H-	H-	Cl-	2-CH_3O-$C_6H_4CH_2NH$-	3.59
49	H-	H-	Cl-	$CH_3(CH_2)_3NH$-	3.37
	Test Set				
T1[c]	$(CH_3)_2C=CH(CH_2CH_2C-(CH_3)=CH)_2CH_2O$-	H-	H-	H-	2.85
T2	3-NO_2-$C_6H_4CH_2O$-	H-	H-	H-	3.53
T3	2, 6-$(F)_2$-$C_6H_3C(=O)O$-	H-	H-	H-	3.36
T4	Cl-	H-	H-	H-	4.45
T5	H-	CH_3O-	HO-	H-	3.71
T6	H-	CH_3O-	HO-	CH_3O-	4.62
T7	H-	NO_2-	Cl-	H-	3.85
T8	H-	H-	Cl-	$C_6H_5C(=O)NH$-	4.42
T9	H-	H-	Cl-	3, 5-$(Cl)_2$-$C_6H_3C(=O)NH$-	3.41
T10	H-	H-	Cl-	2, 6-$(F)_2$-$C_6H_3C(=O)NH$-	3.57

[a] Calculated from eq (2). [b] Furoly group. [c] Farnesyl group.

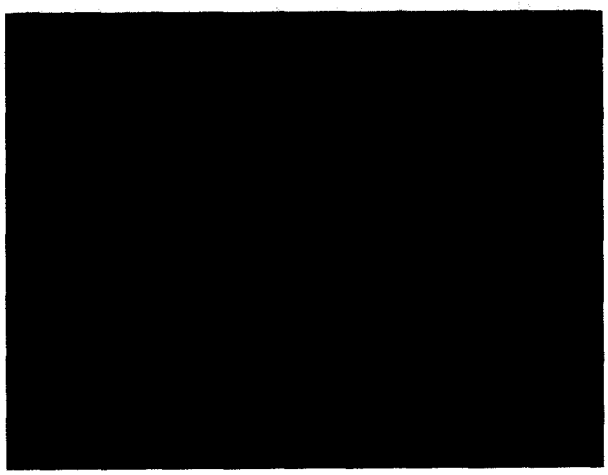

Fig. 1. Superimposed complexes using ligand-based molecular alignment. Atoms with capped sticks type were selected as the fitting fragment.

Computational methods and ligand-based molecular alignment

A grid search was used to find low energy conformers of cinnamaldehyde analogues by systematically changing the dihedral angles of flexible bonds by 30 degree and energy was calculated at each step using a TRIPOS force field with Gasteiger-Hückel charges until the energy gradient converged to below 0.05 kcal/mol. The (θ, φ) dihedral angles of global minimum of the template structure, **1**, had dihedral angles of (156.0°, 179.9°) and its TRIPOS energy was 3.30 kcal/mol. Since no experimental x-ray data were available, the three-dimensional structure of each lowest energy conformer was adopted as an initial structure. A total of 49 ligand structures were selected as a training set and were superimposed to the template structure, **1**, to perform CoMFA analyses. A superimposed image of the 49 ligand structures is shown in Fig. 1. All calculations were done on a SGI octane 2 workstation using SYBYL 6.9 software packages.

PLS analysis using CoMFA with the region focusing method

CoMFA is one of the well-known 3D-QSAR descriptors that has been useful to produce 3D models to indicate the regions that affect biological activity with a change in the chemical substitution (Cho *et al.*, 1996; Huang *et al.*, 2002; Raichurkar *et al.*, 2003; Zhu *et al.*, 2001). CoMFA quantifies the statistical relationship between the 3D properties of a set of small molecules and a global property, such as their potency in a particular biological assay. The steric and electrostatic field energies were calculated using sp^3 carbon probe atoms with a +1 charge. The CoMFA grid spacing used in this work was 2.0Å (Model 1) or 1.0Å (Model 2) in all X, Y, and Z directions. The CoMFA QSAR equations were calculated with the partial least square (PLS) algorithm. The optimal number of components (ONC) in the final PLS model was determined by the r^2_{cv} and standard error of estimate values, obtained from the leave-one-out cross-validation technique. The van der Waals potential and columbic terms, which represent the steric and electrostatic terms, respectively, were calculated using the standard TRIPOS force field. A distance dependent dielectric constant of 1.00 was used. Values of the steric and electrostatic energy were truncated at 30 kcal/mol.

In this work, however, CoMFA with a normal setup gave a cross-validated regression coefficient (r^2_{cv}) of 0.26, which is too low. This suggested that the statistical result might not have any meaning. Region focusing is the application of weights to the lattice points in a CoMFA region to enhance or attenuate the contribution of those points to subsequent analyses when the CoMFA r^2_{cv} value is below some limit (less than 0.5), which was true for in this case (Forina *et al.*, 1999; Lindgren *et al.*, 1994). When the weights are equal to the StDev*Coefficient values, the process is exactly equivalent to the image enhancement of the derived CoMFA maps. The sharpness of focusing is controlled by a user-provided exponential factor. This factor should generally be kept below 1 or too many descriptors will be dropped and r^2_{cv} will fall off. In this work, the coefficient of 0.5 was used for the focusing step. As a result of region focusing, PLS contributions from minor descriptors have been suppressed and the r^2_{cv} has risen.

The partial least-squares (PLS) analysis algorithm was used in conjugation with the cross-validation (leave-one-out) option to obtain an optimum number of components (ONC) that were used to generate the final CoMFA without cross validation. The result from the cross validation analysis was expressed as r^2_{cv} which is defined as

$$r^2_{cv} = 1 - \text{PRESS} / \Sigma(Y_{obs} - Y_{mean})^2$$

where

$$\text{PRESS} = \Sigma (Y_{obs} - Y_{pred})^2$$

PLS analysis using CoMSIA

In order to examine the effects of additional fields except for steric (S) or electrostatic (E) - hydrophobic (H), hydrogen bond donor (D) or acceptor (A), comparative similarity indices analysis (CoMSIA) study was also performed using the same optimized training set molecules as suggested by a referee. A total of five models were tried to include various field effects: Model 3 – using all five fields (SEDHA), Model 4 – using SE fields, Model 5 – using SHE fields, Model 6 – using SEDA fields, Model 7 – using DAH fields. Same grid spacings (1Å or 2.0Å) were used in the CoMSIA analysis.

RESULTS AND DISCUSSION

Determination of the best predicted model and application to the test set using CoMFA

The CoMFA approach was used to elucidate the QSAR as descriptors for FPTase inhibitors with anticancer biological activity. The results obtained from the PLS analysis are summarized in Table II. From this table, we find that r^2_{cv} is 0.557 and 0.474 for Model 1 and Model 2, respectively, and r^2_{ncv} is 0.950 and 0.962 for the respective models. We selected Model 1 as the best predictive CoMFA model because its r^2_{cv} is higher than that of Model 2, (Podlogar *et al.*, 2001) which means that the decrease in the grid spacing was unable to improve the analysis.

The activities of the 49 training set compounds were predicted from the PLS analysis for Model 1 and the results along with the actual pI_{50} values are summarized in Table III. Plots of actual pI_{50} vs. predicted pI_{50} are shown

Table II. The results of PLS analysis in the Training Set using CoMFA.

		Model 1	Model 2
Region Focusing Method		StDev*05[a]	StDev*05[a]
Grid Space		2.0 Å	1.0 Å
PLS Analysis	r^2_{cv}	0.557	0.474
	Components	7	7
	r^2_{ncv}	0.950	0.962
	SEE	0.107	0.093
	F Value	112.01	150.27
Contribution	Steric	0.661	0.585
	Electrostatic	0.339	0.415

[a] StDev*05 means that the region focusing method was applied with the weighting function of StDev*Coefficients and with an exponential factor of 0.5.

Table III. Actual and predicted (Pred.) activities (pI_{50}[a]) and their residuals (Resid.[b]) in the Training Set from CoMFA analysis.

No.	Model 1			Model 2			No.	Model 1			Model 2		
	Actual	Pred.	Resid.	Actual	Pred.	Resid.		Actual	Pred.	Resid.	Actual	Pred.	Resid.
1	2.27	2.45	-0.18	2.27	2.44	-0.17	**26**	3.43	3.44	-0.01	3.43	3.37	0.06
2	3.34	3.29	0.05	3.34	3.24	0.10	**27**	3.19	3.22	-0.03	3.19	3.21	-0.02
3	3.24	3.31	-0.07	3.24	3.35	-0.11	**28**	3.85	3.84	0.01	3.85	3.83	0.02
4	3.44	3.46	-0.02	3.44	3.38	0.06	**29**	3.55	3.63	-0.08	3.55	3.59	-0.04
5	3.30	3.34	-0.04	3.30	3.30	0.00	**30**	3.57	3.55	0.02	3.57	3.57	0.00
6	3.51	3.45	0.06	3.51	3.46	0.05	**31**	3.56	3.67	-0.11	3.56	3.70	-0.14
7	3.49	3.49	0.00	3.49	3.44	0.05	**32**	3.56	3.45	0.11	3.56	3.49	0.07
8	3.27	3.17	0.10	3.27	3.23	0.04	**33**	3.75	3.71	0.04	3.75	3.73	0.02
9	3.38	3.33	0.05	3.38	3.31	0.07	**34**	3.26	3.39	-0.13	3.26	3.33	-0.07
10	3.68	3.72	-0.04	3.68	3.74	-0.06	**35**	2.77	2.56	0.21	2.77	2.58	0.19
11	5.56	5.57	-0.01	5.56	5.57	-0.01	**36**	2.47	2.57	-0.10	2.47	2.47	0.00
12	3.95	3.96	-0.01	3.95	3.92	0.03	**37**	3.44	3.45	-0.01	3.44	3.51	-0.07
13	3.41	3.40	0.01	3.41	3.36	0.05	**38**	3.79	3.86	-0.07	3.79	3.83	-0.04
14	3.57	3.54	0.03	3.57	3.53	0.04	**39**	3.20	3.10	0.10	3.20	3.15	0.05
15	3.03	3.27	-0.24	3.03	3.17	-0.14	**40**	3.02	2.99	0.03	3.02	3.07	-0.05
16	3.37	3.49	-0.12	3.37	3.4	-0.03	**41**	3.70	3.59	0.11	3.70	3.59	0.11
17	3.43	3.41	0.02	3.43	3.44	-0.01	**42**	3.51	3.59	-0.08	3.51	3.58	-0.07
18	3.48	3.43	0.05	3.48	3.45	0.03	**43**	4.17	3.92	0.25	4.17	3.91	0.26
19	3.59	3.53	0.06	3.59	3.57	0.02	**44**	3.51	3.55	-0.04	3.51	3.55	-0.04
20	3.58	3.58	0.00	3.58	3.61	-0.03	**45**	3.55	3.77	-0.22	3.55	3.75	-0.20
21	3.21	3.34	-0.13	3.21	3.33	-0.12	**46**	3.31	3.26	0.05	3.31	3.22	0.09
22	3.62	3.46	0.16	3.62	3.58	0.04	**47**	3.50	3.48	0.02	3.50	3.53	-0.03
23	3.48	3.42	0.06	3.48	3.48	0.00	**48**	3.59	3.69	-0.10	3.59	3.71	-0.12
24	3.58	3.48	0.10	3.58	3.51	0.07	**49**	3.37	3.32	0.05	3.37	3.37	0.00
25	3.62	3.56	0.06	3.62	3.58	0.04							

[a]Calculated from eq (2). [b]Resid.=pI_{50}(Actual)-pI_{50}(Pred.)

in Fig. 2. Close examination of Table III shows that the average residual of the actual and predicted value is only 0.07.

The steric and electrostatic field contributions are 66:34 indicating a slightly superior influence of the formerly mentioned contribution on ligand-receptor interactions. Graphical representations of the steric and electrostatic maps are displayed in Figs. 3 and 4, respectively. For reference, the most active compound **11**, shown in atom type color is displayed in the contour maps. Both maps are quite simple and they concentrated on the R_1 region mainly due to the diverse variations of the *ortho* position compared to the *meta* or *para* position. The sterically favored region (shown in green, contribution level 80%) is shown between the benzyloxy oxygen and *ortho* substituent of the benzyloxy group, whereas three sterically unfavorable regions (shown in yellow, contribution level 20%) are found near the phenyl group or immediately below the sterically favored region. This suggests that most of the R_1 region is not available for a large substituent except for a smaller one: for example, the *ortho*-OCH_3 group in 11 showed the best activity. From the electrostatic contour map shown in Fig. 4, we found that positive charge favored regions (shown in blue, contribution level 80%) are displayed nearly at the same position as the sterically favored region (largely in between the benzyloxy oxygen and *ortho* substituent of the benzyloxy group) and between the R_1 and R_2 positions. However, negative charge favored regions (shown in red, contribution level 20%) are not clearly shown. Again, the electrostatic map is coincided with the methyl group of the *ortho* substituent in the benzoyloxy group.

To validate our calculated results, ten compounds with a pI_{50} range between 2.85 and 4.62 were assigned as a test set and their biological activities were predicted from the PLS results of Model 1 and the results are summarized in Table IV. The average residual is 0.61. Predicted pI_{50} values agree well with the experimental ones, which indicates that our CoMFA approach is valid in explaining differences of biological activities in cinnamaldehyde analogues.

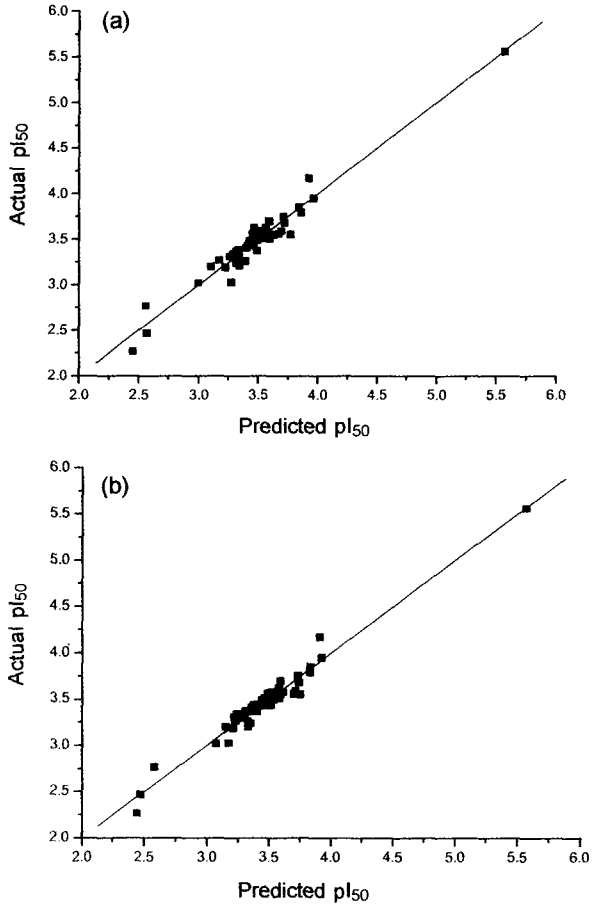

Fig. 2. Comparison of actual vs. predicted pI_{50} using Model 1 (r = 0.975) and Model 2 (r = 0.981)

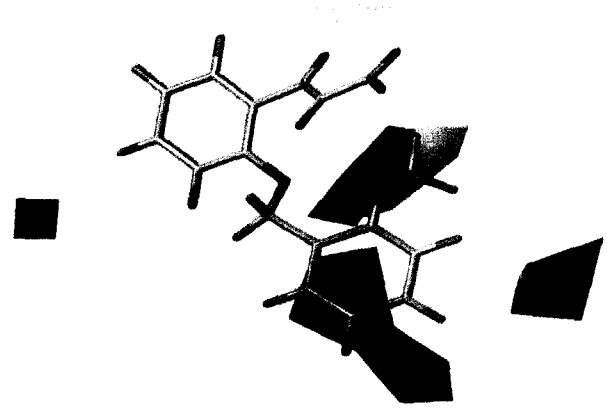

Fig. 3. Superposition of the CoMFA steric stdev*coeff contour plot. Green regions represent sterically favored area. Yellow regions represent sterically disfavored area.

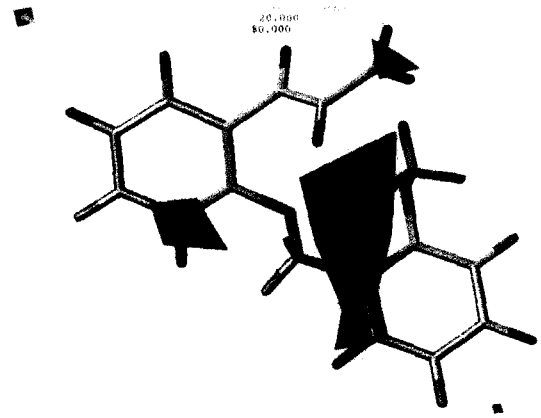

Fig. 4. Superposition of the CoMFA electrostatic stdev*coeff contour plot. Blue regions represent positive charge favored areas. Red regions represent negative charge favored area.

Table IV. Actual and predicted activities (pI_{50}[a]) and their residuals[b] in the Test Set

No.	Model 1			Model 2		
	Actual	Predicted	Residual	Actual	Predicted	Residual
T1	2.85	3.31	-0.46	2.85	3.27	-0.42
T2	3.53	3.42	0.11	3.53	3.42	0.11
T3	3.36	3.72	-0.36	3.36	3.69	-0.33
T4	4.45	3.42	1.03	4.45	3.36	1.09
T5	3.71	2.94	0.77	3.71	2.78	0.93
T6	4.62	3.04	1.58	4.62	3.03	1.59
T7	3.85	3.00	0.85	3.85	3.12	0.73
T8	4.42	3.66	0.76	4.42	3.69	0.73
T9	3.41	3.61	-0.20	3.41	3.61	-0.20
T10	3.57	3.82	-0.25	3.57	3.87	-0.30
		ave.	0.61		ave.	0.61

[a]Calculated from eq (2). [b]Residual=pI_{50}(Actual)-pI_{50}(Predicted)

Prediction based on CoMSIA approach

We have performed the CoMSIA study using five different models by combining different field effects. The r^2_{cv} values were, however, quite low (0.006~0.226) like normal CoMFA results. This suggested that the CoMSIA approach might not reliable. It has been shown that the r^2_{cv} value should be greater than 0.5 to have any statistical significance (Podlogar *et al.*, 2001). Since any other advanced method, such as the region focusing was not applicable to the CoMSIA calculation, we could not improve these results.

CONCLUSION

In order to perform ligand-based QSAR studies, 49 cinnamaldehyde analogues as FPTase inhibitors were superimposed and aligned to investigate three-dimensional steric and electrostatic maps using the CoMFA approach. Two models were generated from the CoMFA approach with the region focusing method. The most predictive model was Model 1 with a grid spacing of 2Å and this model showed good statistical results (r^2_{ncv} =0.950). The CoMFA maps are concentrated on the R_1 position favoring a smaller *ortho* substituent on the benzyloxy group. From above PLS correlations, the activities of the ten test set molecules were predicted satisfactorily. CoMSIA approach, which can consider effects of additional fields did not give any satisfactory results.

ACKNOWLEDGEMENTS

This work was supported by a grant (R11-2002-100-03002-2) from ERC program of the Korea Science and Engineering Foundation. This work was also supported by an INHA UNIVERSITY Research Grant (INHA-31644).

REFERENCES

Adari, H., Lowy, D. R., Willumsen, B. M., Der, C. J., and McCormick, F., Guanosine triphosphate activating protein (GAP) interacts with the p21 ras effector binding domain. *Science*, 240, 518-521 (1988).

Cho, S. J., Garsia, M. L. S., Bier, J., and Tropsha, A., Structure-based alignment and comparative molecular field analysis of acetylcholinesterase inhibitors. *J. Med. Chem.*, 39, 5064-5071 (1996).

Cho, Y. K., CoMFA on Cinnamaldehyde Analogues against FPTase Inhibitory Acitivity, Ph.D. thesis, Graduate school of Chungnam National University, Korea (2002).

Choo, H.-Y. P., Choi, S., Ryu, C.-K., Kim, H.-J., Lee, I. Y., Pae, A. N., and Koh, H. Y., QSAR study of quinolinediones with inhibitory activity of endothelium-dependent vasorelaxation by CoMSIA. *Bioorg. Med. Chem.*, 11, 2019-2023 (2003).

Forina, M., Casolino, C., and Millan, C. P., Iterative predictor weighting (IPW) PLS: a technique for the elimination of useless predictors in regression problems. *J. Chemometr,* 13, 165-184 (1999).

Gibbs, J. B. and Oliff A., Pharmaceutical research in molecular oncology. *Cell*, 79, 193-198 (1994).

Huang, M., Yang, D.-Y., Shang, Z., Zou, J., and Yu, Q., 3D-QSAR studies on 4-hydroxyphenylpyruvate dioxygenase inhibitors by comparative molecular field analysis (CoMFA). *Bioorg. Med. Chem. Lett.*, 12, 2271-2275 (2002).

Knight, D. W., Feverfew: chemistry and biological activity. *Nat. Prod. Rep.*, 12, 271-276 (1995).

Kwon, B. M., Cho, Y. K., and Lee, S. H., 2'-Hydroxycinnamaldehyde from stem bark of *Cinnamomum cassia*. *Planta Medica,* 62, 183-184 (1996).

Kwon, B. M., Lee, S. H., Cho, Y. K., Bok, S. H., So, S. H., Youn, M. R., and Chang, S. I., Synthesis and biological activity of cinnamaldehyde as angiogenesis inhibitors. *Bioorg. Med. Chem. Lett.*, 7, 2473-2476 (1997).

Kwon, B. M., Lee, S. H., Choi, S. U., Park, S. H., Lee, C. O., Cho, Y. K., Sung, N. D., and Bok, S. H., Synthesis and *in vitro* cytotoxicity of cinnamaldehyde to human solid tumor cells. *Arch. Pharm. Res.*, 21, 147-152 (1998).

Lindgren F, Geladi P, Rännar S, and Wold S., Interactive Variable Selection (Ivs) For Pls .1. Theory and Algorithms. *J. Chemometr.*, 8, 349-363 (1994).

Lodish, H., Berk, A., Zipursky, S. L., Matsudaira, P., Baltimore, D., and Darnell, J., Molecular Cell Biology, W. H. Freeman and Company, New York, (1995).

Pedretti, A., Villa, L., and Vistoli, G., Modeling of binding modes and inhibition mechanism of some natural ligands of farnesyl transferase using molecular docking. *J. Med. Chem.*, 45, 1460-1465 (2002).

Podlogar, B. L., Muegge, I., and Brice, L. J., Computational methods to estimate drug development parameters. *Curr. Opin. Drug Discovery Dev.*, 4, 102-109 (2001).

Qian, Y., Blaskovich, M. A., Saleem, M., Seong, C. M., Wathen, S. P., Hamilton, A. D., and Sebti, S. M., Design and structural requirements of potent peptidomimetic inhibitors of p21ras farnesyltransferase, *J. Biol. Chem.*, 269, 12410-12413 (1994).

Raichurkar, A. V. and Kulkarni, V. M., Understanding the antitumor activity of novel hydroxysemicarbazide derivatives as ribonucleotide reductase inhibitors using CoMFA and CoMSIA. *J. Med. Chem.*, 46, 4419-4427 (2003).

Reiss, Y., Goldstein J. L., Seabra, M. C., Casey, P. J., and Brown, M. S., Inhibition of purified $p21^{ras}$ farnesyl:protein transferase by Cys-AAX tetrapeptides. *Cell*, 62, 81-88 (1990).

Schweins, T., Geyer, M., Scheffzek, K., Warshel, A., Kalbitzer, H. R., and Wittinghofer, A., Substrate-assisted catalysis as a mechanism for GTP hydrolysis of p21ras and other GTP-binding proteins. *Nat. Struct. Biol.*, 2, 36-44 (1995).

Sung, N.-D., Cheun, Y. G., Kwon, B.-M., Park, H.-Y., and Kim, C. K., Modeling of inhibition mechanism of natural ligands to farnesyl protein transferase using molecular docking. *Bull. Kor. Chem. Soc.*, 24, 1509-1511 (2003).

Wu, T.-S., Ou, L.-F., and Teng, C.-M., Aristolochic acids, aristolactam alkaloids and amides from *Aristolochia kankauensis*. *Phytochemistry*, 36, 1063-1068 (1994).

Zhu, L., Hou, T., and Xu, X., Three-dimensional quantitative structure-activity relationship study on paullones as CDK inhibitors using CoMSIA and CoMFA. *J. Mol. Model.*, 7, 223-230 (2001).